

# MHz-Band Near-field Coupling Communication Technology

Kohei Nagata, Tomoaki Yanagawa, Tatsuya Kusunoki\*,  
Ryuki Shimoda, Hitoshi Shimasaki, Yuichi Kado  
Department of Electronics, Kyoto Institute of Technology  
Kyoto, Japan  
+81-75-724-7451  
Kado@kit.ac.jp

## ABSTRACT

We have proposed the MHz-band near field coupling communication technology using the surface of the human body as a communication path between the TRX on the surface of the human body (Wearable TRX) and the TRX embedded in the environment (Embedded TRX). This is called human area networking technology, and it has allowed "Touch and Connect" intuitive form of communication. In order to apply this technology to medical field, we embedded the transceiver (In-body TRX) in the phantom which has the same electrical characteristics with the human body, and we measured the packet error rate (PER) between the In-body TRX and the Wearable TRX. Additionally, we assessed the coverage around the human body by measuring the PER between the Wearable and the Embedded TRXs. We found from the results that our MHz-band near field coupling system was applicable to a single system of communication between In-body, Wearable, and Embedded TRXs.

## Categories and Subject Descriptors

B.4.1 [INPUT/OUTPUT AND DATA COMMUNICATIONS]:  
Data Communications Devices – *Receivers. Transmitters.*

B.4.4 [INPUT/OUTPUT AND DATA COMMUNICATIONS]:  
Performance Analysis and Design Aids – *Verification.*

B.4.5 [INPUT/OUTPUT AND DATA COMMUNICATIONS]:  
Reliability, Testing, and Fault-Tolerance – *Error-checking.*

## General Terms

Measurement, Experimentation, Human Factors, Verification.

## Keywords

Near-field coupling communication, Human-Area networking, Transmission characteristics, Packet error rate

## 1. INTRODUCTION

Wireless body area networks around the human body are expected to play an important role in various areas of application,

such as in the remote monitoring of health, sports training, interactive gaming, sharing of personal information, security authentication, train ticket wickets, and medical information systems [1]. Body-channel communication (BCC) has recently been studied [2]–[6]. This is communication between TRXs on the surface of the human body (Wearable TRXs), which uses the human body as the communication path. However, we proposed human-area networking technology based on near field coupling communication (NFCC) that consists of Wearable TRXs and a transceiver embedded in environments (Embedded TRX) [7]–[9]. NFCC provides more versatile systems than BCC, and enables intuitive communication through "Touch and Connect". We also focus on medical applications using this technology.

Fig. 1 shows a model for medical applications. A TRX embedded in the human body (In-body TRX) collects health information and communicates with the Wearable TRX outside the body, so that we can monitor information at all times. Moreover, we can combine healthcare over the network by using NFCC between the Embedded TRX connected to the network and the Wearable TRX. The advantages of NFCC are its short radial distance and low power consumption. Consequently, we can limit the influence of medical equipment such as pacemakers in hospital scenarios, and can prevent health information from being leaked. In addition, we can use it long-term without having to replace batteries.

Using Wearable TRXs with personal information enables us to know where patients are located and the condition of their health. Furthermore, improved security is accomplished; for example, only a person who has a Wearable TRX can open doors.

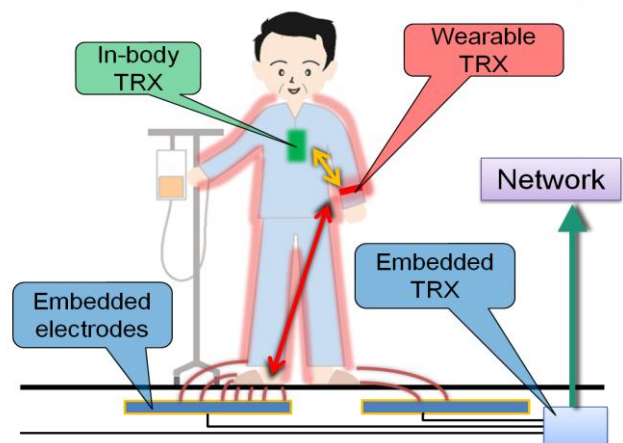


Figure 1. Model of scenario in medical applications

\* Presently at Sumitomo Electric Industries. Ltd., Osaka Japan.

## 2. COMMUNICATION MODEL

NFCC consists of three types of TRXs, i.e., In-body, Wearable, and Embedded TRXs. The In-body TRX is assumed to be a device embedded in the human body that checks health information. The Wearable TRX is attached to the surface of the human body, like a watch, to be used as monitoring equipment.

Communication is carried out between the In-body and Wearable TRX, and also between the Wearable and Embedded TRX. Both the In-body and Wearable TRX use the same TRX. The Embedded TRX is assumed to be embedded in walls or floors.

The communication model between the In-body and the Wearable TRX is outlined in Fig. 2, and the communication model between the Wearable and Embedded TRX and between the Wearable TRXs is outlined in Fig. 3. When modulated signals are applied to a pair of parallel electrodes implemented in the Wearable TRX, a quasi-electrostatic field is generated near the electrodes. An electrical field signal is induced on the human body through a mechanism for near-field coupling. The signal loop is composed of two types of paths. The first is a forward path and the second is a return path. From Figs. 2 and 3, the forward path is a route from the electrode of the Wearable or the In-body TRX on the body side (signal electrode) to the electrode of the Embedded or the Wearable TRX on the body side through the human body's surface. In contrast, the return path is a route that returns again from the ground electrode to the electrode of the Wearable or the In-body TRX through the earth grounding.

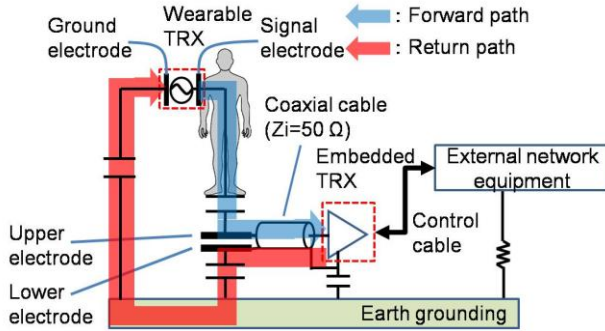


Figure 2. Communication path between Wearable and Embedded TRX

The direction of communication from the Wearable to the Embedded TRX and the In-body to the Wearable TRX is called the uplink in Figs. 2 and 3. In contrast, the inverse of each direction of communication is called a downlink.

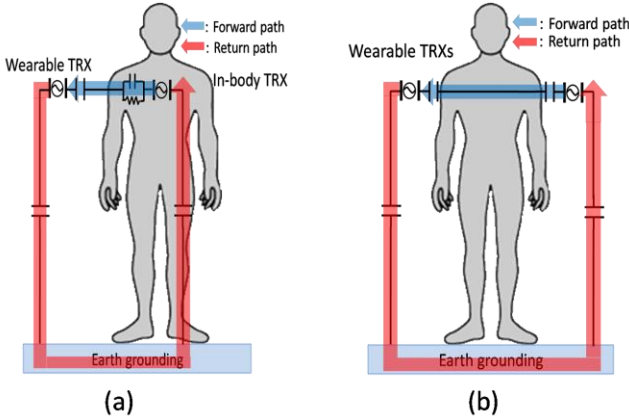
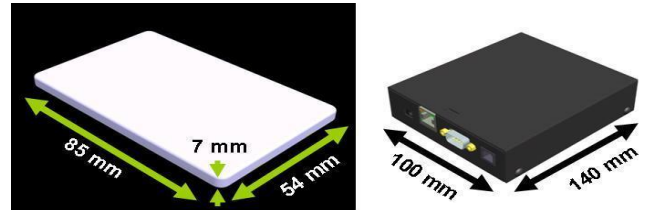


Figure 3. Communication paths between In-body TRX and Wearable TRX, and Wearable TRXs

## 3. TRX CONFIGURATION

We fabricated a Wearable and an Embedded TRX that could be installed into various objects in our surroundings, such as doors, floors, PCs, and equipment. Fig. 4 has photographs of the configurations for the TRXs. The prototype used a 6.75 MHz carrier frequency and binary phase-shift keying (BPSK) and it achieved a transmission rate of 420 kbps. The Wearable TRX was mainly composed of a multi-chip module (MCM), a power circuit, and a coin battery. It could operate for approximately one year on a single CR3032 button-type lithium-ion battery and incorporated electrically erasable programmable read-only memory (EEPROM), which could be used to store user data for applications. We used two different output voltages when we used the Wearable TRX. The first was the "Normal V<sub>out</sub>" of 8 V, and the second was the "Double V<sub>out</sub>" of 16 V. The Embedded TRX was mainly composed of MCM, filters, input amplifiers, a transmitter driver, an RS232C driver, and power circuits. Its power supply was 5 V and it provided an RS232C communication interface for connection to external devices. The electrodes for the Embedded TRX were connected by a coaxial cable to the SubMiniature version A (SMA) connector of the TRX.



Wearable TRX		Embedded TRX	
Supply voltage	3.0 V	Supply voltage	6.0 V
Bitrate	420 kbps	Bitrate	420 kbps
Carrier frequency	6.75 MHz	Carrier frequency	6.75 MHz
		Interface	RS232C

Figure 4. Configuration and basic specifications for TRX

## 4. MEASUREMENT OF PER

### 4.1 Experimental System

There is a schematic of the configuration of the system to measure packet error rate (PER) in Fig. 5. We used a phantom that had the same electrical properties as those of the human body to ensure the measurements of PER could be reproduced.

The phantom was made of water-absorbing gel that absorbed saline solution. The phantom's dimensions were 95 x 19 x 19 cm, and its conductivity was 0.59 S/m at 6.75 MHz (human body: 0.60 S/m) [10], which was the carrier frequency of NFCC. The Wearable TRX was set up around the phantom because it was assumed to be the peripheral device around the body. The In-body TRX was the same as the Wearable TRX and was embedded in the phantom because it was assumed to be a device embedded in the body. The In-body TRX used Normal V<sub>out</sub>. The Embedded TRX was connected to electrodes embedded in the floor (350-mm-sqr.) with coaxial cable because it was assumed the TRX was embedded in the environment. In addition, the Embedded TRX was connected to a desktop PC with RS232C cable. A rubber sheet, which was 5 x 350 x 350 mm, was inserted between the phantom and embedded electrodes and between the embedded electrodes and floor. We inserted a common-mode choke coil

between the Embedded TRX and embedded electrodes to suppress noise. The total length of packet data was 22 bytes. Each packet consisted of an address, data, and commands. Ten thousand packets were sent at 1-ms interval. After all the packets had been sent, we confirmed the number that had successfully been received. We also calculated PER.

We measured PER between the In-body and the Wearable TRX and between the Wearable and Embedded TRX. When In-body TRX communicates with Wearable TRX in actual use, there are interspaces between the human body and the Wearable TRX. Polystyrene boards (0~80 mm) were placed between the phantom and the Wearable TRX to reproduce this situation and vary the distance between them. We reproduced the depth at which the In-body TRX was embedded in the human body by varying embedding depth in the phantom. Polystyrene boards were similarly placed between the Wearable and Embedded TRX in communication. TRXs that were the same as the Wearable TRX were simultaneously placed on the side of the phantom (upper and lower RX) and we measured PER between the Wearable TRX and RXs. The RXs were assumed to be devices that are mounted on the surface of the human body.

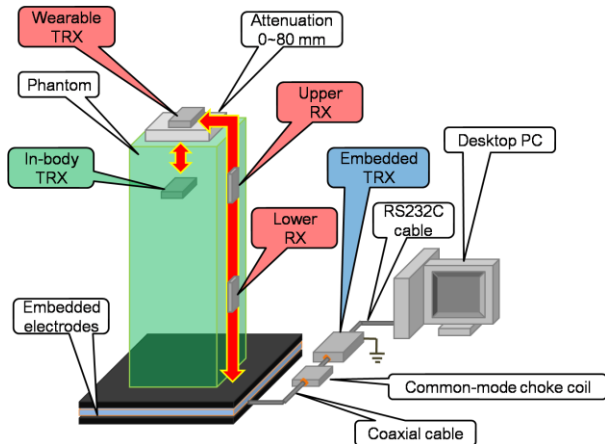


Figure 5. Schematic of PER measurements

## 4.2 Results

Fig. 6 plots PER in communication from the In-body to the Wearable TRX. The greater the distance between the phantom and the Wearable TRX or the In-body TRX, the more PER worsens.

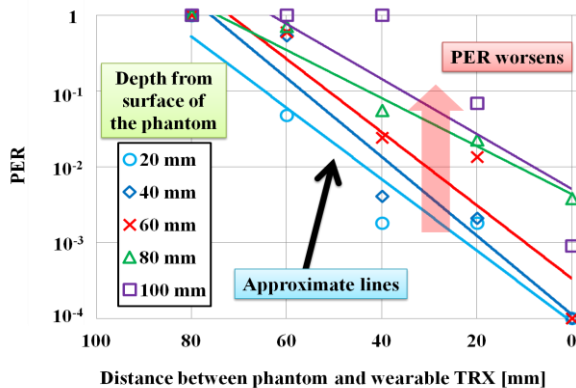


Figure 6. PER from In-body to Wearable TRX

Fig. 7 plots PER in communication from the Wearable to the In-body TRX when the measurements used normal  $V_{out}$  or double

$V_{out}$ . The dotted lines plot normal  $V_{out}$ , and the solid lines plot double  $V_{out}$ . Compared with Figs. 6 and 7, we found that the quality of the communication from the Wearable to the In-body TRX was worse than that of backward communication. When we used normal  $V_{out}$  in these measurements, no communication was established at any Wearable TRX-phantom distances between 20 to 80 mm. However, communication was established at distances between 0 to 60 mm when we used double  $V_{out}$ .

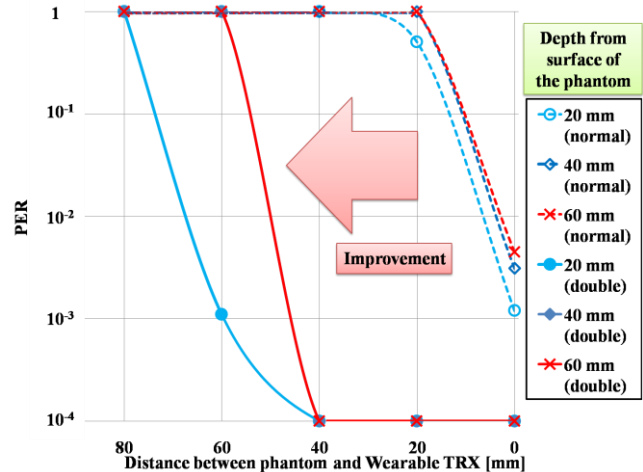


Figure 7. PER from Wearable to In-body TRX

Fig. 8 shows a simulation of the electric field distribution around the phantom. Fig. 8 (a) indicates the electric field generated by the In-body TRX and Fig. 8 (b) indicates the electric field generated by the Wearable TRX. According to Fig. 8, the range of communication from the Wearable to the In-body TRX is narrower than that of backward communication. These results coincided with those we obtained from measurements. The output voltages of the In-body and the Wearable TRX were 4.4 V in this simulation and their signal frequency was 6.75 MHz. The size and the electrical properties of the box placed at the center were the same as those of the phantom.

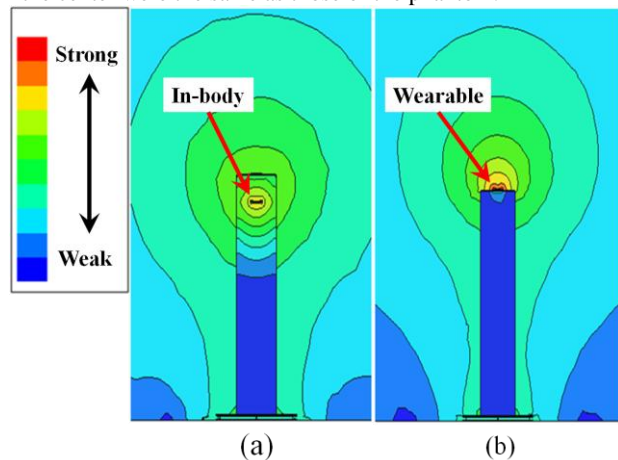


Figure 8. (a) Electric distribution from In-body TRX

(b) Electric distribution from Wearable TRX

Fig. 9 plots PER in communication from the Wearable TRX to the upper RX or the lower RX or Embedded TRX. In communication to the upper RX and lower RX, despite the distance between the Wearable TRX and the phantom, the PER was more than  $10^{-2}$  when we used normal  $V_{out}$ . Communication was possible below 40 mm in the upper RX communication.

However, when we used double  $V_{out}$ , communication was established below 80 mm. For Embedded TRX, the results of all measurements were error free for both normal  $V_{out}$  and double  $V_{out}$ . Finally, although not shown in this figure, the results for all measurements of communication from the Embedded TRX to the Wearable TRX were error free.

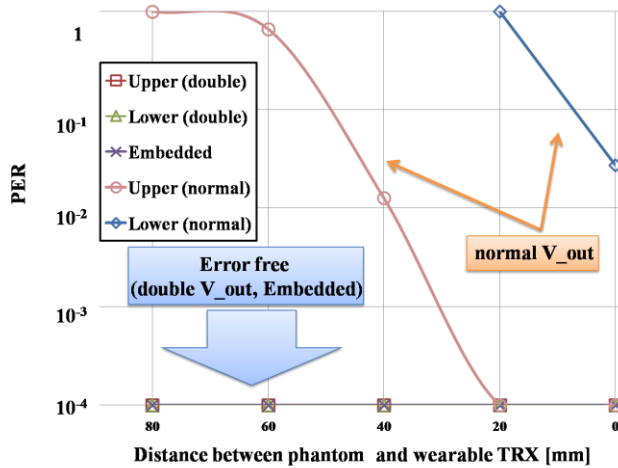


Figure 9. PER from Wearable TRX to Embedded TRX and RXs

## 5. CONCLUSION

We studied the human-area networking technology based on near field coupling mechanism and explored the possibility of expanding this communication system around humans by applying this technology to communication inside the human body. As a result, we ensured that it was possible to apply the frequency of 6.75 MHz used in NFCC to provide a single system of communication between In-body, Wearable, and Embedded TRXs. Therefore, we found the feasibility of using communication based on NFCC operating as a medical information system by using peripheral devices on the human body. We intend to determine the optimum output voltage and miniaturize In-body TRXs in the future. Moreover, improvements in convenience and security over communication network around and inside the human body are expected by using this technology.

## 6. ACKNOWLEDGMENTS

Part of this work was supported by a Grant-in-Aid for Scientific Research (A) 23246073 from the Ministry of Education, Culture, Sports, Science and Technology of Japan.

## 7. REFERENCES

- [1] M. Chen, et. al., "Body Area Networks: A Survey," *Mobile Networks and Applications*, Vol. 16, No. 2, pp. 171–193, Spring 2011.
- [2] Y. Kado, "Human-Area Network Technology as a Universal Interface," *Symp. on VLSI Circuit Digest of Technical Papers*, pp. 102–105, 2009.
- [3] T. G. Zimmerman, "Personal Area Networks: Near-field intrabody communication," *IBM Syst. J.*, Vol. 35, Nos. 3–4, pp. 609–617, 1996.
- [4] N. Cho, et. al., "The Human Body Characteristics as a Signal Transmission Medium for Intrabody Communication," *IEEE Trans. MTT*, Vol. 55, pp. 1080–1086, May 2007.
- [5] S. J. Song, N. Cho, S. Kim, J. Yoo, S. Choi, and H. J. Yoo, "A 0.9 V 2.6 mW Body-Coupled Scalable PHY Transceiver for Body Sensor Applications," *IEEE ISSCC*, pp. 366–367, Feb. 2008.
- [6] A. Fazzi, S. Ouzonov, and J. V. D. Homberg, "A 2.75 mW Wideband Correlation-Based Transceiver for Body-Coupled Communication," *IEEE ISSCC*, pp. 204–205, Feb. 2009.
- [7] M. Sinagawa, et. al., "A near-field-sensing transceiver for intrabody communication based on the electro-optic effect," *IEEE Trans. Instrum. Meas.*, Vol. 53, No. 6, pp. 1533–1538, 2004.
- [8] Y. Kado and M. Shinagawa, "AC Electric Field Communication for Human-Area Networking," *IEICE Trans. Electron*, Vol. E93–C, pp. 234–243, Mar. 2011.
- [9] Y. Kado, et. al., "Human-Area Networking Technology Based on Near-Field Coupling Transceiver," *Proc. of IEEE Radio & Wireless Symposium (RWS2012)*, pp. 119–122.
- [10] S. Gabriel, R.W.Lau and C. Gabriel, "The dielectric properties of biological tissues: II. Measurements in the frequency range 10 Hz to 20 GHz", *Phys. Med. Biol.* Vol.41, pp.2251-2269, 1996